PROCEEDINGS OF SPIE

SPIEDigitalLibrary.org/conference-proceedings-of-spie

The CARMENES M-dwarf planet survey

Quirrenbach, Andreas, Consortium, CARMENES

Andreas Quirrenbach, CARMENES Consortium, "The CARMENES M-dwarf planet survey," Proc. SPIE 11447, Ground-based and Airborne Instrumentation for Astronomy VIII, 114473C (13 December 2020); doi: 10.1117/12.2561380

Event: SPIE Astronomical Telescopes + Instrumentation, 2020, Online Only

The CARMENES M-dwarf planet survey

A. Quirrenbach[a], P. J. Amado[b], I. Ribas[c,d], A. Reiners[e], J. A. Caballero[f], J. Aceituno[b,g], J. M. Alacid[f], F. J. Alonso-Floriano[h], G. Anglada-Escudé[c,d], M. Azzaro[g], D. Baroch[c,d], F. F. Bauer[b], S. Becerril[b], V. J. S. Béjar[i,j], P. Bluhm[a], R. Calvo Ortega[b], C. Cardona Guillén[i,j], N. Casasayas-Barris[i,j], P. Chaturvedi[k], C. Cifuentes[f], J. Colomé[c,d], D. Cont[e], M. Cortés-Contreras[f], S. Czesla[l], E. Díez-Alonso[m], A. J. Domínguez Fernández[n], S. Dreizler[e], C. Duque-Arribas[n], N. Espinoza[o], B. Fuhrmeister[l], D. Galadí-Enríquez[g], E. García Quintana[c,d], E. González-Álvarez[p], L. González Cuesta[i,j], J. I. González Hernández[i,j], E. W. Guenther[k], E. de Guindos[g], A. P. Hatzes[k], T. Henning[q], O. Herbort[r,e], E. Herrero[c,d], D. Hintz[l], J. Iglesias-Páramo[b,g], S. V. Jeffers[s,e], E. N. Johnson[e], E. de Juan[g], A. Kaminski[a], J. Kemmer[a], J. Khaimova[e], S. Khalafinejad[a], H. Klahr[q], D. Kossakowski[q], L. Kreidberg[q], M. Kürster[q], F. Labarga[n], M. Lafarga[c,d], M. Lampón[b], L. M. Lara[b], J. Lillo-Box[f], N. Lodieu[i,j], Á. López Gallifa[n], M. J. López González[b], M. López-Puertas[b], R. Luque[i,j], E. Marfil[n], S. Martín-Ruiz[b], C. Matthé[a], K. Molaverdikhani[a,q], D. Montes[n], J. C. Morales[c,d], M. Morales-Calderón[f], E. Nagel[k,l], L. Nortmann[e], G. Nowak[i,j], A. Ofir[t], M. Oshagh[i,j], E. Pallé[i,j], V. M. Passegger[u,l], A. Pavlov[q], S. Pedraz[g], V. Perdelwitz[v], M. Perger[c,d], S. Reffert[a], D. Revilla[n], E. Rodríguez[b], C. Rodríguez López[b], S. Sabotta[a,k], S. Sadegi[a,q], L. Sairam[w,l], M. Salz[l], A. Sánchez-López[h], J. Sanz-Forcada[f], P. Sarkis[q], S. Schäfer[e], J. Schiller[k], M. Schlecker[q], J. H. M. M. Schmitt[l], P. Schöfer[e], A. Schweitzer[l], W. Seifert[a], Y. Shan[e], D. Shulyak[s,e], S. L. Skrzypinski[n], E. Solano[f], M. G. Soto[x], O. Stahl[a], M. Stangret[i,j], S. A. Stock[a], J. B. P. Strachan[y], T. Stuber[a], J. Stürmer[a], H. M. Tabernero[z], L. Tal-Or[v], M. Tala-Pinto[a], T. Trifonov[q], S. Vanaverbeke[aa], F. Yan[e], M. R. Zapatero Osorio[p], and M. Zechmeister[e]

[a]Landessternwarte, Zentrum für Astronomie der Universität Heidelberg, Königstuhl 12, D-69117 Heidelberg, Germany
[b]Instituto de Astrofísica de Andalucía (CSIC), Glorieta de la Astronomía s/n, E-18008 Granada, Spain
[c]Institut de Ciències de l'Espai (ICE, CSIC), Campus UAB, c/ de Can Magrans s/n, E-08193 Bellaterra, Barcelona, Spain
[d]Institut d'Estudis Espacials de Catalunya (IEEC), E-08034 Barcelona, Spain
[e]Institut für Astrophysik, Georg-August-Universität Göttingen, Friedrich-Hund-Platz 1, D-37077 Göttingen, Germany
[f]Centro de Astrobiología (CSIC-INTA), Campus ESAC, Camino Bajo del Castillo s/n, E-28692 Villanueva de la Cañada, Madrid, Spain
[g]Centro Astronómico Hispano-Alemán (MPG-CSIC), Observatorio Astronómico de Calar Alto, Sierra de los Filabres, E-04550 Gérgal, Almería, Spain
[h]Leiden Observatory, Leiden University, Postbus 9513, 2300 RA, Leiden, The Netherlands
[i]Instituto de Astrofísica de Canarias, c/ Vía Láctea s/n, E-38205 La Laguna, Tenerife, Spain
[j]Departamento de Astrofísica, Universidad de La Laguna, E-38206 Tenerife, Spain
[k]Thüringer Landessternwarte Tautenburg, Sternwarte 5, D-07778 Tautenburg, Germany
[l]Hamburger Sternwarte, Gojenbergsweg 112, D-21029 Hamburg, Germany
[m]Instituto Universitario de Ciencias y Tecnologías Espaciales de Asturias, c/ Independencia 13, E-33004 Oviedo, Spain

Ground-based and Airborne Instrumentation for Astronomy VIII, edited by Christopher J. Evans, Julia J. Bryant, Kentaro Motohara, Proc. of SPIE Vol. 11447, 114473C · © 2020 SPIE · CCC code: 0277-786X/20/$21 · doi: 10.1117/12.2561380

[n]Departamento de Física de la Tierra y Astrofísica & IPARCOS-UCM (Instituto de Física de Partículas y del Cosmos de la UCM), Facultad de Ciencias Físicas, Universidad Complutense de Madrid, E-28040 Madrid, Spain
[o]Space Telescope Science Institute, 3700 San Martin Drive, Baltimore, MD, USA
[p]Centro de Astrobiología (CSIC-INTA), Campus INTA, Carretera de Ajalvir km 4, E-28850 Torrejón de Ardoz, Madrid, Spain
[q]Max-Planck-Institut für Astronomie, Königstuhl 17, D-69117 Heidelberg, Germany
[r]SUPA, School of Physics & Astronomy, University of St. Andrews, St. Andrews, KY16 9SS, United Kingdom
[s]Max Planck Institute for Solar System Research, Justus-von-Liebig-Weg 3, D-37077 Göttingen, Germany
[t]Department of Earth and Planetary Sciences, Weizmann Institute of Science, Rehovot 76100, Israel
[u]Homer L. Dodge Department of Physics and Astronomy, University of Oklahoma, 440 West Brooks Street, Norman, OK 73019, United States of America
[v]Department of Physics, Ariel University, Ariel 40700, Israel
[w]School of Physics & Astronomy, University of Birmingham, Edgbaston, Birmingham B15 2TT, United Kingdom
[x]Departamento de Astronomía, Universidad de Chile, Camino de El Observatorio 1515, Las Condes, Santiago, Chile
[y]School of Physics and Astronomy, Queen Mary University London, 327 Mile End Road, London E1 4NS, United Kingdom
[z]Instituto de Astrofśica e Ciências do Espa co, Universidade do Porto, CAUP, Rua das Estrelas, 4150-762 Porto, Portugal
[aa]Centre for mathematical Plasma-Astrophysics, Department of Mathematics, KU Leuven, Celestijnenlaan 200B, 3001 Heverlee, Belgium

ABSTRACT

The CARMENES instrument consists of two cross-dispersed échelle spectrographs, which together cover the wavelength range from 5,200 to 17,100 Å. During its first five years of operation at the 3.5 m telescope on Calar Alto, Spain, it has been used for a radial-velocity survey of 365 M dwarfs, for follow-up radial-velocity observations of transiting exoplanets, and for spectroscopic studies of exoplanet atmospheres during transits. The CARMENES data have also yielded a wealth of information on the fundamental parameters and activity of M dwarfs. We provide an overview of the scientific results from the main CARMENES survey in the years 2016 to 2020.

Keywords: Spectrographs, Optical Instrumentation, Near-Infrared Instrumentation, Extrasolar Planets, Cool Stars, M Dwarfs

1. INTRODUCTION

Our census of planetary systems in the Solar neighborhood, and our understanding of their formation, could not be complete without systematic searches for planets orbiting M dwarfs. In fact, this spectral type encompasses a large range of masses from the hydrogen burning limit at $0.07\,M_\odot$ to about $0.6\,M_\odot$, and thus a great variety of stellar properties (see Sect. 3.2). Since three out of four stars in the disk of the Milky Way belong to this type, it is quite possible that our closest neighbors live on a planet orbiting an M dwarf – provided that these objects are

Further author information: E-mail: A.Quirrenbach@lsw.uni-heidelberg.de, Telephone: +49 6221 541792

hospitable for life at all. An operational definition of the "habitable zone" around a star is given by the separation range where liquid water can exist on the surface of rocky planets. For the low-luminosity M dwarfs, this zone is rather close to the star, corresponding to orbital periods of just a few weeks or even days. This, together with the low stellar mass, facilitates searches for habitable-zone planets with the radial-velocity (RV) technique, as the signal K scales with the stellar mass M_* and the orbital period P according to $K \propto M_*^{-2/3} P^{-1/3}$. Here we report on the CARMENES survey, which is currently obtaining precise RVs of 365 M dwarfs at the 3.5 m telescope of the Centro Astronómico Hispano-Alemán (CAHA) at Calar Alto (Almería, Spain).

2. THE CARMENES INSTRUMENT

2.1 Instrument Concept, Design, and Construction

The CARMENES instrument was designed specifically for a large M-dwarf radial velocity survey with the 3.5 m telescope on Calar Alto, as described in Sect. 3. An initial study (Quirrenbach et al. 2010) concluded that an instrument with resolution $R \approx 85,000$ covering the wavelength range $0.5\,\mu\text{m} \leq \lambda \leq 1.35\,\mu\text{m}$ (with a goal to extend this range to $1.7\,\mu$m) would be optimum for this purpose. This led to a design with two independent cross-dispersed échelle spectrographs for the visible (VIS) and near-IR (NIR) ranges (Seifert et al. 2012; Quirrenbach et al. 2014), coupled to the telescope by optical fibers (Stürmer et al. 2014). All CARMENES partner institutions (see acknowledgements below) contributed to the construction of the instrument hardware and software (Pérez-Calpena et al. 2016; García-Vargas et al. 2016), and a large room in the dome of the 3.5 m telescope was prepared for the installation of the two spectrograph vacuum tanks and the auxiliary equipment (Helmling et al. 2016). After a short integration and verification phase (Becerril et al. 2016; Seifert et al. 2016), CARMENES saw "first light" on the sky on Nov. 9, 2015, and entered scientific operations on Jan. 1, 2016 (Quirrenbach et al. 2016).

2.2 Data Analysis

The first steps in the processing of CARMENES data are carried out by the `caracal` pipeline (Caballero et al. 2016b). These include applying standard corrections for detector bias and dark current, tracing the échelle orders on the detector, extracting the one-dimensional spectra, and performing the wavelength calibration. The resulting fully reduced spectra from both spectrographs are then analyzed with a second pipeline, `serval` (Zechmeister et al. 2018). For each observation, this program computes the RV by cross-correlating the observed spectrum with a reference template constructed from all observed spectra of the same star. Further small corrections to the observed RVs are applied as described by Trifonov et al. (2018). In addition, `serval` provides a number of spectral line indices, which are useful tools to diagnose stellar variability, and to distinguish it from Keplerian signals due to planetary companions. For the same purpose, `serval` also computes indicators of the differential line width (dLW), and of the wavelength dependence of the RV (chromatic index, CRX).

An alternative way of computing RV time series is through cross-correlation with a binary mask constructed from synthetic spectra. This is frequently done for earlier-type stars, but more difficult for M dwarfs because of the complexity of their spectra. Nevertheless, RVs with a precision approaching that of the standard data reduction have also been generated with the binary mask method (Lafarga et al. 2020), which also gives absolute RVs suitable e.g. for determining the space velocities of the target stars.

2.3 Instrument Performance

During the commissioning and initial operation phases of CARMENES, basic performance parameters such as throughput and spectral resolution were established. It turned out that hollow-cathode lamps are suitable for precise wavelength calibration, but their spectra contain a number of lines of neon or argon that are so bright that the lamps cannot be used in simultaneous exposures with stars. The calibration procedures were therefore modified to use simultaneous star and Fabry-Pérot etalon exposures in combination with a cross-calibration between the etalons and hollow-cathode lamps during daytime (Quirrenbach et al. 2018).

The suitability of RV time series for planet searches is limited mainly by three factors: the intrinsic instability of the stellar atmosphere, photon noise, and the stability of the spectrograph. The CARMENES survey targets show RV "jitter" due to activity and star spots, with a broad distribution around a median of ~ 3 m/s. For most of these stars, the SNR obtained with integration times of up to 20 min is sufficient to achieve a contribution

≤ 2 m/s from photon noise to the RV precision of the VIS spectra (Quirrenbach et al. 2018). A detailed analysis of the thermal behavior of the spectrograph, along with the calibration and data reduction procedures, shows that the median instrumental precision in the VIS channel is 1.2 m/s (Bauer et al. 2020). This value can probably be even lowered by future improvements in the thermal environment of the instrument. The CARMENES M dwarf survey is thus limited mainly by the intrinsic RV stability of the stars, except for the faintest targets (mostly stars of spectral type M5 and later), for which the performance is limited by photon noise.

The NIR RV data from the survey have substantially larger scatter. This is mostly due to the fact that the information content of M star spectra in this wavelength range is substantially lower than in the visible (Reiners et al. 2018b), leading to poorer photon-noise limited performance. With longer integration times, it should be possible to get close to the instrument limit of 2.4 m/s (Bauer et al. 2020), but this is rarely done within the survey program.

3. THE CARMENES RADIAL-VELOCITY SURVEY

The CARMENES M-dwarf survey has been the largest program at the Calar Alto 3.5 m telescope from 2016 to 2020, with more than 18,500 VIS and nearly 18,000 NIR spectra obtained in about 5,000 hours of observing time. Most of this time has been devoted to a "blind" survey of nearby M dwarfs (Sect. 3.1); about 400 hours were dedicated to follow-up observations of transiting planets (Sect. 3.4). The telescope operations and data taking were performed by the observatory staff, supported by an automated scheduling system (Garcia-Piquer et al. 2017).

3.1 The M Star Sample

The CARMENES survey sample consists of 365 stars. The selection criteria were chosen such that they cover all spectral subtypes of the M class (Quirrenbach et al. 2012). CARMENES has a performance "sweet spot" in the M3-M4 subtype range: for these stars CARMENES is more sensitive than spectrographs working at bluer wavelengths (such as HARPS and HARPS-N), and there are many bright stars, for which high-SNR spectra can be obtained with integration times not exceeding 20 minutes. For the later spectral subtypes, all stars at declination $\delta \geq -23°$ that are sufficiently bright to allow a good RV measurement are covered by the survey. Here a slightly reduced precision, and integration times of up to 30 minutes, were accepted to enlarge the sample size. This selection excludes "problematic" stars such as close binaries, in which contamination by the secondary spectrum could corrupt the RV determination. Early M dwarfs are included in the sample to enable statistical analyses of the exoplanet population for host star masses in a large range from the hydrogen burning limit at $0.07\,M_\odot$ all the way up to $0.6\,M_\odot$. Conveniently, the set of early M dwarfs also serves as a pool of bright poor-weather targets. No pre-selection on activity indicators, rotation period, $v \sin i$, or metallicity was done, so as to enable investigations of relations between stellar activity indicators, precise RV measurements, and other time series with the CARMENES data. While the survey targets do not constitute a volume-limited sample, the very simple selection criteria (essentially the brightest stars with $\delta \geq -23°$ in each spectral sub-type) have been adopted to facilitate a statistical census of planets in the Solar neighborhood – the average distance of the CARMENES stars is only 13 pc.

3.2 Properties of M Dwarfs

Early on in the project, the "Carmencita" data base was created with the goal of compiling all relevant information on a "parent sample", from which the CARMENES survey stars could be selected (Caballero et al. 2016a). Carmencita currently holds exhaustive information on 2202 stars, based on literature searches, our own observations carried out in preparation for the CARMENES survey, and analyses of CARMENES data. The preparatory program included multi-band photometry (Díez Alonso et al. 2019; Cifuentes et al. 2020), high-resolution imaging (Cortés-Contreras et al. 2017), low-resolution spectroscopy (Alonso-Floriano et al. 2015), as well as high-resolution spectroscopy (Jeffers et al. 2018).

CARMENES VIS and NIR spectra of 324 stars were made public in an early science release (Reiners et al. 2018b), comprising the largest homogeneous collection of high-resolution spectra of M dwarfs. The photospheric parameters T_{eff}, $\log g$, and metallicity (represented by [Fe/H]) of most target stars have been determined by fitting synthetic PHOENIX-ACES models to the observed spectra (Passegger et al. 2018, 2019). A deep learning approach was used to derive the same parameters along with $v \sin i$ (Passegger et al. 2020). The most serious difficulty here is the "synthetic gap", i.e., the qualitative difference in the number and distribution of spectral features included in synthetic and real spectra. Work on more detailed abundance analyses based on CARMENES spectra is still in its infancy, but the work on the neutron-capture elements Rb, Sr, and Zr by Abia et al. (2020) shows the potential of using high-resolution, high-SNR spectra of M dwarfs for studies of the chemical evolution of the Galaxy.

In the context of exoplanet surveys, mass and radius are the most important stellar parameters, as they enter measurements of the corresponding planetary properties from RVs and transit light curves directly. Reliable estimates of M_* and R_* for all CARMENES stars are now available, thanks to a combination of the mentioned spectroscopic analyses with multi-band photometry and with astrometry from the *Gaia* and *Hipparcos* missions (Schweitzer et al. 2019). Nine new double-lined spectroscopic binaries found in the CARMENES data by Baroch et al. (2018) will contribute to the underlying mass calibration, once their spectroscopic orbital elements can be supplemented with the inclination from *Gaia* astrometry.

Magnetic fields permeate the photospheres and chromospheres of cool stars, and affect individual spectra as well as time series in many direct and indirect ways. Tal-Or et al. (2018) showed that RV variations of the stars with RV scatter of > 10 m/s and a projected rotation velocity $v \sin i > 2$ km/s are caused mainly by activity. An analysis of Zeeman broadening in Ti I and FeH lines in the CARMENES NIR spectra of these stars showed that they indeed all have fields with strengths of a few kG (Shulyak et al. 2019). The RV variations, along with their chromatic behavior can be modeled well with active regions (i.e., spots and regions with modified convection properties) rotating in and out of view (Baroch et al. 2020).

The most conspicuous signature of stellar activity are emission lines. In the spectral range covered by CARMENES, Hα, Paβ, He I D_3, the Na I D doublet, the Ca II infrared triplet (IRT), and the He I triplet at 10,830 Å probe mostly the chromosphere, while TiO and VO band indices provide information about the photosphere (Schöfer et al. 2019). The temperature structure of the chromosphere, and the filling factor of active regions, can be inferred from modeling of the emission lines (Hintz et al. 2019, 2020), while wing asymmetries and their temporal evolution can be used to infer vertical motions and to test their connection to flares (Fuhrmeister et al. 2018). In some cases, it is also possible to determine the rotation period from variable emission lines (Fuhrmeister et al. 2019b). Understanding the strength and temporal behavior of emission lines such as He I λ10,830 as investigated by Fuhrmeister et al. (2019a, 2020) is also important in the context of planetary transmission spectroscopy (Sect. 4.1 and 4.2), as unrecognized variability of the stellar line can completely invalidate the analysis of the stellar spectrum.

3.3 Planets of M Dwarfs

Among the first stars scheduled for CARMENES observations were a number of M dwarfs with known planets. As a result, we were able to verify the RV performance of the instrument, and to refine the previously derived orbits. In addition, the combination of the CARMENES data with pre-existing data sets led to the discovery of two new giant planets, GJ 1148 c and GJ 15 Ac (Trifonov et al. 2018). These were soon followed by the first Neptune-mass planets whose existence could be established on the basis of CARMENES data alone, HD 147379 b (Reiners et al. 2018a) and HD 180617 b (Kaminski et al. 2018). In both cases, archival data from HIRES, and in the latter case also from HARPS, could be included in the orbital solution. The discoveries of the warm super-Earths GJ 3779 b and GJ 1265 b by Luque et al. (2018), and of a 3.2 $M_\oplus$ companion to Barnard's Star by Ribas et al. (2018), marked the first successes with respect to the core CARMENES science case of finding rocky planets of low-mass stars.

The increasing number of spectra taken as the survey proceeded has enabled further discoveries of planets with masses in the super-Earth to Neptune range (Nagel et al. 2019; Perger et al. 2019; Lalitha et al. 2019; González-Álvarez et al. 2020; Bauer et al. 2020; Stock et al. 2020b). So far, 22 new planets have been discovered by the "blind" CARMENES survey. Taken together, they constitute a good fraction of the planets known around M dwarfs (see also Fig. 1). More importantly, because of the simple and well-known selection criteria of the CARMENES survey, this sample provides a solid basis for statistical analyses exploring the properties of the intermediate-mass planet population as a function of host star mass. At the low end of this range, $M_* \leq 0.1$ $M_\odot$, the Trappist-1 system is now joined by the two companions of Teegarden's Star (Zechmeister et al. 2019). They

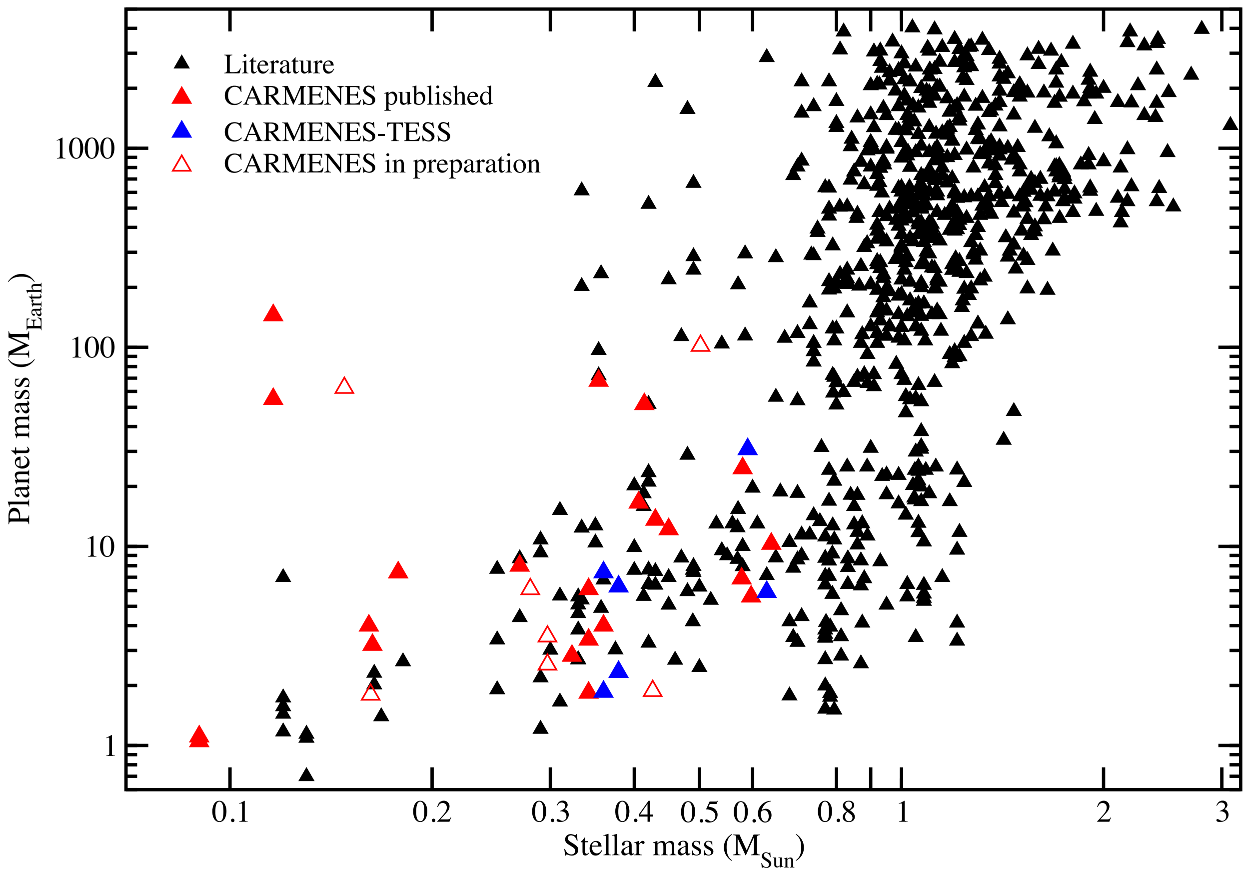

Figure 1. Planets discovered by the "blind" CARMENES survey (red) and from the CARMENES-TESS program (blue) in the context of all planets with dynamical masses determined with RVs. More than 40% of the known planets with host masses $\leq 0.2\,M_\odot$ are CARMENES discoveries.

furnish evidence that systems with multiple Earth-like planets are very common around ultra-cool dwarf stars – otherwise we would have been extremely lucky twice to get discoveries from rather small target samples. With nearly equal masses $m \sin i = 1.1\,M_\oplus$ and insolation of 0.37 and 1.15 times the terrestrial value, the planets of Teegarden's Star count among the most "Earth-like" known, albeit with a very non-Solar host. Because of their proximity (3.8 pc), they may be the best objects for studies of Earth analogs in extreme environments with future space-based mid-infrared interferometers.

Another CARMENES discovery of note is GJ 3512 b (Morales et al. 2019), the highest-mass planet known with a low-mass ($M_* \leq 0.3\,M_\odot$) host. With $m \sin i = 0.46\,M_{Jup}$, it challenges the standard paradigm of planet formation through core accretion, because a high migration rate is expected for rocky cores forming in the disks of stars with such low mass. Further information for investigations of links between planet formation an migration scenarios on one hand, and architectures of mature systems on the other hand, can be gleaned from multiple systems. This usually requires RV monitoring over a long time and with a large number of individual observations, as exemplified by the two-planet system GJ 1148 (Trifonov et al. 2020) and the three planets orbiting YZ Cet (Stock et al. 2020a). The latter case also demonstrates that a correct identification of the dynamical state of the system is possible only if aliases of the true orbital periods with the sampling function of the RV time series (usually dominated by multiples of a Solar or siderial day) can successfully be resolved.

3.4 Masses of Transiting Planets

Follow-up observations of transiting planets with RV measurements are particularly valuable, as the combined information – radius and inclination from the transits, and mass from the RVs – yields the bulk density of the planet, and thus a first rough constraint on its internal composition. RV observations of transiting planets with CARMENES have concentrated mostly on M star hosts, taking full advantage of the red-infrared wavelength range covered by the instrument. In the past few years, suitable targets have become available through the *K2* extension of the *Kepler* mission, and in particular from *TESS*. Because of their proximity, objects such as the Earth-sized hot planet GJ 357 b (Luque et al. 2019b) are among the best-suited for future spectroscopic studies with the *James Webb Space Telescope* and ground-based extremely large telescopes.

In the mass range between Earth and Neptune, there is no tight universal mass-radius relation. The broad distribution of observed radii at any mass implies a large diversity in composition, ranging from objects such as K2-18 b with a mass of $m = 9\,\mathrm{M}_\oplus$ and density $\rho \sim 4\,\mathrm{g\,cm^{-3}}$, hinting at the presence of a volatile-rich envelope (Sarkis et al. 2018), to K2-292 b, which is very dense with $\rho \sim 7.4\,\mathrm{g\,cm^{-3}}$ in spite of its rather high mass of $m = 24.5\,\mathrm{M}_\oplus$ (Luque et al. 2019a). Again, multiple systems are of particular interest, as one and the same star may host planets with rather different densities (Palle et al. 2019; Hidalgo et al. 2020). As an added bonus, RV follow-up of transiting planets has the potential to reveal additional non-transiting planets, clarifying the system architecture (Luque et al. 2019b; Kemmer et al. 2020). Planets in sparsely populated areas of the parameter space, such as LP 714-47 b in the "hot Neptune desert" (Dreizler et al. 2020) are key for exploring the interplay of accretion, migration and mass-loss in their formation.

The distribution of planets in the four-dimensional [mass – radius – host star mass – orbital separation] space also holds important clues on their formation and evolution. The two-dimensional sub-space [radius – insolation] is of special interest in the context of planetary atmospheres and of processes leading to their loss, including photo-evaporation. Objects such as the super-Earth TOI-1235 b (Bluhm et al. 2020), and the system LTT 3780 with an inner planet of Earth-like composition and an outer sub-Neptune (Nowak et al. 2020), help to characterize the gap between rocky and gas-dominated planets, which is currently not defined very well for low-mass hosts.

4. TRANSIT SPECTROSCOPY

4.1 Atomic and Molecular Spectroscopy

Whereas CARMENES was designed and optimized explicitly as a radial-velocity instrument, it is also well-suited for transit spectroscopy of planetary atmospheres due to its combination of excellent stability, high spectral resolving power, and wide wavelength coverage. These characteristics enable studies of individual lines including the Na I D doublet, Hα, the K I D1 line, and the Ca II IRT. Since all of these lines are also strong in the stellar atmospheres, great care has to be exercised, however, to model the wavelength-dependent center-to-limb darkening and the Rossiter-McLaughlin effect along with the planetary spectrum, as pointed out by Casasayas-Barris et al. (2020), who find that the signatures of these lines seen in transit spectra of HD 209458 can possibly be explained entirely by stellar effects.

While individual molecular lines are too weak to be detectable in planetary atmospheres during transits, the presence of molecular bands can be probed through cross-correlation with a suitable template. Applying this technique to CARMENES-NIR spectra, water vapor has been found in HD 189733 b (Alonso-Floriano et al. 2019a) and HD 209458 b (Sánchez-López et al. 2019). In both cases, the peak of the cross-correlation function is blueshifted with respect to the planetary rest frame, indicating the presence of day- to night-side winds at the terminators of these hot Jupiters. The relative strengths of different water bands are affected by atmospheric hazes. The fact that the water bands in the 7,000 to 9,600Å range are detected in CARMENES-VIS transit spectra of HD 209458 b, but not of HD 189733 b, can thus be explained by the presence of high-altitude hazes in the latter planet, which are largely absent in the former (Sánchez-López et al. 2020).

Ultra-hot Jupiters with equilibrium temperatures well in excess of 2,000 K have recently garnered widespread interest. Yan et al. (2019) detected the Ca II H and K lines and the IRT in transit spectra of WASP-33 b and KELT-9 b from HARPS-N and CARMENES, demonstrating the complementarity of the two instruments, which cover the blue and the far-red, respectively. The lines are deeper than expected, which is probably the result of a hydrodynamic outflow that transports a significant amount of Ca^+ into the upper atmosphere. A high mass-loss rate and a thermospheric temperature of $\sim 12,000$ K are inferred from the hydrogen Balmer lines in WASP-33 b by Yan et al. (2020), who again combined HARPS-N and CARMENES data.

In a different approach, Oshagh et al. (2020) used spectra from HARPS, CARMENES-VIS and CARMENES-NIR to exploit the wavelength dependence of the Rossiter-McLaughlin effect in the full range from 3,800 to 17,100 Å as a probe of the atmosphere of HD 189733 b. The consistency between the resulting broad-band transmission spectrum and the one derived from *Hubble Space Telescope* data demonstrates the potential of this technique for ground-based investigations of hazy atmospheres.

4.2 Evaporating Planets

During the first years of its existence, CARMENES was unique in providing access to the near-infrared spectral region, including of course the He I triplet at 10,830 Å, with a stabilized high-resolution spectrograph. This capability was exploited by pioneering studies of extended helium atmospheres in several planets including the Saturn-mass planet WASP-69 b (Nortmann et al. 2018). In this planet, blueshifts of the He absorption of several km/s and post-transit absorption were observed; this can be interpreted as the escape of part of the atmosphere trailing behind the planet in comet-like form.

Strong He I absorption is also detected in the hot Jupiter HD 189733 b, albeit without clear pre- or post-transit absorption, which could indicate material beyond the planetary Roche lobe, or radial velocities in excess of the escape velocity (Salz et al. 2018). Weaker detections have also been obtained in HD 209458 b (Alonso-Floriano et al. 2019b) and GJ 3470 b (Palle et al. 2020). It appears that stellar activity and the level of XUV irradiation have a strong influence on the detectability of an absorption signal. This is expected as the metastable 2^3S helium triplet state, which is the lower level of the observed absorption lines, is populated via radiative ionization of neutral He by photons with wavelengths < 504 Å followed by recombination. More detailed hydrodynamical models can be employed to infer the structure and temperature of the thermosphere, and to estimate the mass loss rate (Lampón et al. 2020).

5. FUTURE PERSPECTIVES

The CARMENES M-dwarf survey will be continued as a CAHA legacy project with 300 observing nights from 2021 through 2023. The instrument will also be used for a separate legacy survey of K dwarfs, and it is open for proposals from the Spanish and international communities, as it has been in the past. The legacy survey will focus primarily on completing the core "blind" survey with at least 50 observations for each star. This will enable a sound statistical assessment of the planet occurrence rates in the host star range from 0.07 to 0.6 $M_\odot$, down to planet masses approaching 1 $M_\oplus$, preferentially in short-period orbits. This survey will be highly complementary to samples from transit surveys, which are even more strongly biased towards short periods and yield radii instead of masses, and to the astrometric census from *Gaia*, which will be sensitive mostly to giant planets with periods of a few years. The M-dwarf legacy project will also include a shallower survey of additional stars in search of analogues to the GJ 3512 system, and characterization of planetary atmospheres through transit spectroscopy. In parallel, various upgrades of the hardware, calibration procedures, and data reduction pipeline are foreseen.

ACKNOWLEDGMENTS

CARMENES is an instrument at the Centro Astronómico Hispano-Alemán (CAHA) at Calar Alto (Almería, Spain), operated jointly by the Junta de Andalucía and the Instituto de Astrofísica de Andalucía (CSIC). The authors wish to express their sincere thanks to all members of the Calar Alto staff for their expert support of the instrument and telescope operations. CARMENES was funded by the Max-Planck-Gesellschaft (MPG), the Consejo Superior de Investigaciones Científicas (CSIC), the Ministerio de Economía y Competitividad (MINECO) and the European Regional Development Fund (ERDF) through projects FICTS-2011-02, ICTS-2017-07-CAHA-4, and CAHA16-CE-3978, and the members of the CARMENES Consortium (Max-Planck-Institut für Astronomie, Instituto de Astrofísica de Andalucía, Landessternwarte Königstuhl, Institut de Ciències de l'Espai, Institut für Astrophysik Göttingen, Universidad Complutense de Madrid, Thüringer Landessternwarte Tautenburg, Instituto de Astrofísica de Canarias, Hamburger Sternwarte, Centro de Astrobiología and Centro Astronómico Hispano-Alemán), with additional contributions by the MINECO, the Deutsche Forschungsgemeinschaft through the Major Research Instrumentation Program and Research Unit FOR2544 "Blue Planets around Red Stars", the Klaus Tschira Stiftung, the states of Baden-Württemberg and Niedersachsen, and by the Junta de Andalucía. This work is based on data from the CARMENES data archive at CAB (CSIC-INTA).

References

Abia, C., Tabernero, H. M., Korotin, S. A., et al. 2020, A&A, 642, A227

Alonso-Floriano, F. J., Morales, J. C., Caballero, J. A., et al. 2015, A&A, 577, A128

Alonso-Floriano, F. J., Sánchez-López, A., Snellen, I. A. G., et al. 2019a, A&A, 621, A74

Alonso-Floriano, F. J., Snellen, I. A. G., Czesla, S., et al. 2019b, A&A, 629, A110

Baroch, D., Morales, J. C., Ribas, I., et al. 2020, A&A, 641, A69

Baroch, D., Morales, J. C., Ribas, I., et al. 2018, A&A, 619, A32

Bauer, F. F., Zechmeister, M., Kaminski, A., et al. 2020, A&A, 640, A50

Becerril, S., Cárdenas, C., Amado, P., et al. 2016, in Society of Photo-Optical Instrumentation Engineers (SPIE) Conference Series, Vol. 9910, Observatory Operations: Strategies, Processes, and Systems VI, ed. A. B. Peck, R. L. Seaman, & C. R. Benn, 99100Q

Bluhm, P., Luque, R., Espinoza, N., et al. 2020, A&A, 639, A132

Caballero, J. A., Cortés-Contreras, M., Alonso-Floriano, F. J., et al. 2016a, in 19th Cambridge Workshop on Cool Stars, Stellar Systems, and the Sun (CS19), 148

Caballero, J. A., Guàrdia, J., López del Fresno, M., et al. 2016b, in Society of Photo-Optical Instrumentation Engineers (SPIE) Conference Series, Vol. 9910, Observatory Operations: Strategies, Processes, and Systems VI, ed. A. B. Peck, R. L. Seaman, & C. R. Benn, 99100E

Casasayas-Barris, N., Pallé, E., Yan, F., et al. 2020, A&A, 635, A206

Cifuentes, C., Caballero, J. A., Cortés-Contreras, M., et al. 2020, A&A, 642, A115

Cortés-Contreras, M., Béjar, V. J. S., Caballero, J. A., et al. 2017, A&A, 597, A47

Díez Alonso, E., Caballero, J. A., Montes, D., et al. 2019, A&A, 621, A126

Dreizler, S., I., J., et al. 2020, arXiv e-prints, arXiv:2011.01716

Fuhrmeister, B., Czesla, S., Hildebrandt, L., et al. 2019a, A&A, 632, A24

Fuhrmeister, B., Czesla, S., Hildebrandt, L., et al. 2020, A&A, 640, A52

Fuhrmeister, B., Czesla, S., Schmitt, J. H. M. M., et al. 2018, A&A, 615, A14

Fuhrmeister, B., Czesla, S., Schmitt, J. H. M. M., et al. 2019b, A&A, 623, A24

Garcia-Piquer, A., Morales, J. C., Ribas, I., et al. 2017, A&A, 604, A87

García-Vargas, M. L., Caballero, J., Pérez-Calpena, A., et al. 2016, in Society of Photo-Optical Instrumentation Engineers (SPIE) Conference Series, Vol. 9911, Modeling, Systems Engineering, and Project Management for Astronomy VI, ed. G. Z. Angeli & P. Dierickx, 99110P

González-Álvarez, E., Zapatero Osorio, M. R., Caballero, J. A., et al. 2020, A&A, 637, A93

Helmling, J., Wagner, K., Hernández Castaño, L., et al. 2016, in Society of Photo-Optical Instrumentation Engineers (SPIE) Conference Series, Vol. 9908, Ground-based and Airborne Instrumentation for Astronomy VI, ed. C. J. Evans, L. Simard, & H. Takami, 99086B

Hidalgo, D., Pallé, E., Alonso, R., et al. 2020, A&A, 636, A89

Hintz, D., Fuhrmeister, B., Czesla, S., et al. 2019, A&A, 623, A136

Hintz, D., Fuhrmeister, B., Czesla, S., et al. 2020, A&A, 638, A115

Jeffers, S. V., Schöfer, P., Lamert, A., et al. 2018, A&A, 614, A76

Kaminski, A., Trifonov, T., Caballero, J. A., et al. 2018, A&A, 618, A115

Kemmer, J., Stock, S., Kossakowski, D., et al. 2020, A&A, 642, A236

Lafarga, M., Ribas, I., Lovis, C., et al. 2020, A&A, 636, A36

Lalitha, S., Baroch, D., Morales, J. C., et al. 2019, A&A, 627, A116

Lampón, M., López-Puertas, M., Lara, L. M., et al. 2020, A&A, 636, A13

Luque, R., Nowak, G., Pallé, E., et al. 2019a, A&A, 623, A114

Luque, R., Nowak, G., Pallé, E., et al. 2018, A&A, 620, A171

Luque, R., Pallé, E., Kossakowski, D., et al. 2019b, A&A, 628, A39

Morales, J. C., Mustill, A. J., Ribas, I., et al. 2019, Science, 365, 1441

Nagel, E., Czesla, S., Schmitt, J. H. M. M., et al. 2019, A&A, 622, A153

Nortmann, L., Pallé, E., Salz, M., et al. 2018, Science, 362, 1388

Nowak, G., Luque, R., Parviainen, H., et al. 2020, A&A, 642, A173

Oshagh, M., Bauer, F. F., Lafarga, M., et al. 2020, A&A, 643, A64

Palle, E., Nortmann, L., Casasayas-Barris, N., et al. 2020, A&A, 638, A61

Palle, E., Nowak, G., Luque, R., et al. 2019, A&A, 623, A41

Passegger, V. M., Bello-García, A., Ordieres-Meré, J., et al. 2020, A&A, 642, A22

Passegger, V. M., Reiners, A., Jeffers, S. V., et al. 2018, A&A, 615, A6

Passegger, V. M., Schweitzer, A., Shulyak, D., et al. 2019, A&A, 627, A161

Pérez-Calpena, A., Seifert, W., Amado, P., et al. 2016, in Society of Photo-Optical Instrumentation Engineers (SPIE) Conference Series, Vol. 9911, Modeling, Systems Engineering, and Project Management for Astronomy VI, ed. G. Z. Angeli & P. Dierickx, 991120

Perger, M., Scandariato, G., Ribas, I., et al. 2019, A&A, 624, A123

Quirrenbach, A., Amado, P. J., Caballero, J. A., et al. 2014, in Society of Photo-Optical Instrumentation Engineers (SPIE) Conference Series, Vol. 9147, Ground-based and Airborne Instrumentation for Astronomy V, ed. S. K. Ramsay, I. S. McLean, & H. Takami, 91471F

Quirrenbach, A., Amado, P. J., Caballero, J. A., et al. 2016, in Society of Photo-Optical Instrumentation Engineers (SPIE) Conference Series, Vol. 9908, Ground-based and Airborne Instrumentation for Astronomy VI, ed. C. Evans, L. Simard, & H. Takami, 990812

Quirrenbach, A., Amado, P. J., Mandel, H., et al. 2010, in Society of Photo-Optical Instrumentation Engineers (SPIE) Conference Series, Vol. 7735, Ground-based and Airborne Instrumentation for Astronomy III, ed. I. S. McLean, S. K. Ramsay, & H. Takami, 773513

Quirrenbach, A., Amado, P. J., Ribas, I., et al. 2018, in Society of Photo-Optical Instrumentation Engineers (SPIE) Conference Series, Vol. 10702, Ground-based and Airborne Instrumentation for Astronomy VII, ed. C. Evans, L. Simard, & H. Takami, 107020W

Quirrenbach, A., Amado, P. J., Seifert, W., et al. 2012, in Society of Photo-Optical Instrumentation Engineers (SPIE) Conference Series, Vol. 8446, Ground-based and Airborne Instrumentation for Astronomy IV, ed. I. S. McLean, S. K. Ramsay, & H. Takami, 84460R

Reiners, A., Ribas, I., Zechmeister, M., et al. 2018a, A&A, 609, L5

Reiners, A., Zechmeister, M., Caballero, J. A., et al. 2018b, A&A, 612, A49

Ribas, I., Tuomi, M., Reiners, A., et al. 2018, Nature, 563, 365

Salz, M., Czesla, S., Schneider, P. C., et al. 2018, A&A, 620, A97

Sánchez-López, A., Alonso-Floriano, F. J., López-Puertas, M., et al. 2019, A&A, 630, A53

Sánchez-López, A., López-Puertas, M., Snellen, I. A. G., et al. 2020, A&A, 643, A24

Sarkis, P., Henning, T., Kürster, M., et al. 2018, AJ, 155, 257

Schöfer, P., Jeffers, S. V., Reiners, A., et al. 2019, A&A, 623, A44

Schweitzer, A., Passegger, V. M., Cifuentes, C., et al. 2019, A&A, 625, A68

Seifert, W., Sánchez Carrasco, M. A., Xu, W., et al. 2012, in Society of Photo-Optical Instrumentation Engineers (SPIE) Conference Series, Vol. 8446, Ground-based and Airborne Instrumentation for Astronomy IV, ed. I. S. McLean, S. K. Ramsay, & H. Takami, 844633

Seifert, W., Xu, W., Stahl, O., et al. 2016, in Society of Photo-Optical Instrumentation Engineers (SPIE) Conference Series, Vol. 9908, Ground-based and Airborne Instrumentation for Astronomy VI, ed. C. J. Evans, L. Simard, & H. Takami, 990865

Shulyak, D., Reiners, A., Nagel, E., et al. 2019, A&A, 626, A86

Stock, S., Kemmer, J., Reffert, S., et al. 2020a, A&A, 636, A119

Stock, S., Nagel, E., Kemmer, J., et al. 2020b, A&A, 643, A112

Stürmer, J., Stahl, O., Schwab, C., et al. 2014, in Society of Photo-Optical Instrumentation Engineers (SPIE) Conference Series, Vol. 9151, Advances in Optical and Mechanical Technologies for Telescopes and Instrumentation, ed. R. Navarro, C. R. Cunningham, & A. A. Barto, 915152

Tal-Or, L., Zechmeister, M., Reiners, A., et al. 2018, A&A, 614, A122

Trifonov, T., Kürster, M., Zechmeister, M., et al. 2018, A&A, 609, A117

Trifonov, T., Lee, M. H., Kürster, M., et al. 2020, A&A, 638, A16

Yan, F., Casasayas-Barris, N., Molaverdikhani, K., et al. 2019, A&A, 632, A69

Yan, F., Wyttenbach, A., Casasayas-Barris, N., et al. 2020, arXiv e-prints, arXiv:2011.07888

Zechmeister, M., Dreizler, S., Ribas, I., et al. 2019, A&A, 627, A49

Zechmeister, M., Reiners, A., Amado, P. J., et al. 2018, A&A, 609, A12